

## Signal Amplification of Self-Potential Biosensor for Glucose Monitoring

Jingyi Chen, Chao Zhou, Hongyu Liu, Ping Li, Yonghai Song and Fugang Xu\*

Key Laboratory of Functional Small Organic Molecule, Ministry of Education, Key Laboratory of Chemical Biology, Jiangxi Province, College of Chemistry and Chemical Engineering, Jiangxi Normal University, Nanchang 330022, China.

\*E-mail: [fgxu@jxnu.edu.cn](mailto:fgxu@jxnu.edu.cn)

Received: 17 July 2015 / Accepted: 25 August 2015 / Published: 30 September 2015

---

A self-powered electrochemical sensor (SPS) has been designed for sensitive detection of glucose based on the glucose oxidase (GOD)/polyvinyl ferrocene (PVF)/ poly(diallyldimethylammonium chloride) (PDDA –reduced graphene oxide (RGO))/glassy carbon electrode (GCE) as a bioanode and bilirubin oxidase (BOD)/PDDA-RGO/GCE as a biocathode. The signal amplification of electron mediator in the electrochemical anode has been investigated in details. The results exhibited that the electron mediator did amplify the signal of SPS and the mediator existed on the surface of electrode was better than that existed in a solution. The electrodes constructed under the optimal conditions have been used to develop a glucose SPS which showed a wide linear range from 0.1 mM to 10 mM ( $R^2 = 0.997$ ) and a low detection limit of 23.7  $\mu\text{M}$  ( $S/N=3$ ). Therefore, the newly developed SPS was sensitive and facile for glucose detection, which could promise the possibility of its application in real samples.

---

**Keywords:** self-powered electrochemical sensor, signal amplification, electron mediator, glucose oxidase

### 1. INTRODUCTION

Quantitative determination of glucose concentration is an issue of great importance in daily life because glucose is one of the most widely distributed saccharides in nature and one of the most important carbohydrates.[1-5] It is living cell energy source and metabolic intermediate in organism. People ingest glucose from food to maintain life activities. While elevated glucose level in blood will damage nerves and blood vessels and then pave the way for heart disease, diabetes mellitus and stroke.[6-11] Therefore, there is an urgent demand for a fast and reliable glucose sensor. Among these

previously developed methods, electrochemical sensor has attracted wide attentions due to its high sensitivity, easy operation and low cost.[12-16]

Over the past few years, electrochemical sensors have achieved great achievements based on the development of nanomaterials.[17-20] Various nanomaterials with good catalytic activity including metal, bimetal, metallic oxide, carbon and composite nanostructures have been developed as electroactive materials to construct electrochemical nonenzymatic glucose sensor.[21-25] However, these nanomaterials could easily aggregate on electrode surface and fall off from the electrode. Besides, most of nonenzymatic glucose sensors were carried out at high potential under alkaline reaction conditions, which limited their direct application for glucose detection in blood. Many organic compounds would make interference to glucose detection at high potential. Enzymatic glucose sensors showed remarkable catalytic ability, high selectivity and fast response under mild conditions.[26-30] For example, a glucose biosensor used in phosphate buffer solutions (PBS, 0.2 M, pH 7.0) was developed based on the three-dimensional (3D) porous carbon electrodes as a support materials to immobilize glucose oxidase (GOD).[31] It was used to detect glucose in blood without any pretreatment and showed high selectivity and nice stability. However, general enzymatic glucose biosensors always were carried out at about -0.5 V based on the reduction of O<sub>2</sub>. At such negative potential, many organic compounds mentioned above would also make interference to glucose detection. Furthermore, the performance of enzymatic glucose biosensors strongly depended on the amount of O<sub>2</sub> in the solution.

Self-powered sensors (SPSs) are composed of a bioanode and a biocathode to provide the power for the sensing events without external applied voltage.[32-35] The SPSs sense analytes on the basis of chemical-to-electrochemical energy transformations in which the power output provides the analytical signal because the power density or open circuit potential (OCP) depend largely on the concentration of the analytes. Since no external voltage is applied to the two electrodes, the SPSs show very high selectivity. As the system is self-powered by biological fluids, the SPSs can also be implanted in body as an invasive sensing device. To date, many kinds of self-powered platforms have been constructed for chemical and biological sensing.[12,34,36-40] Willner and co-workers firstly described a glucose SPSs with an anode consisting of glucose oxidase (GOD) reconstituted on a flavin adenine dinucleotide-modified monolayer and a layered crosslinked cytochrome c/cytochrome oxidase cathode.[41] Kakehi et al. developed a miniaturized glucose SPSs integrated with a wireless system in 2007. [42] In 2011, Dong's group firstly introduced the logic concept into SPSs to propose the first self-powered logic enzymatic biosensor.[36] Although a lots of SPSs have been developed, the sensitivity of the SPSs was always neglected which is vital issue.

In this work, a SPS was developed for glucose sensing by using GOD/polyvinyl ferrocene (PVF)/poly(diallyldimethylammonium chloride) (PDDA)-reduced graphene oxide (RGO)/glassy carbon electrode (GCE) as a bioanode and bilirubin oxidase (BOD)/PDDA-RGO/GCE as a biocathode, respectively. The effect of electron mediator on signal amplification of SPSs has been explored in detail.

## 2. EXPERIMENTAL SECTION

### 2.1. Materials

GOD (EC 1.1.3.4, 140 U mg<sup>-1</sup>), BOD (5.6 U mg<sup>-1</sup>) and PDDA (MW 200000-350000, 35 wt%) were obtained from Sigma-Aldrich. Graphite powder (99.95%, 325 mesh) was purchased from Aladdin Ltd (Shanghai, China). Ferrocene (Fc), polyvinyl ferrocene (PVF) and some other reagents were purchased from Beijing Chemical Reagent Factory (Beijing, China). The PBS (0.2 M) was prepared by mixing 0.2 M NaH<sub>2</sub>PO<sub>4</sub> and 0.2 M Na<sub>2</sub>HPO<sub>4</sub>. The GOD solution (10 mg/mL) and BOD solution (5 mg/mL) were prepared in 0.2 M PBS (pH 7.0), respectively. Ultra-pure water purified by a Millipore-Q System ( $\rho \geq 18.2$  M $\Omega$  cm) was used whole experiments.

### 2.2 Fabrication of PDDA-RGO nanocomposites

Graphene oxide (GO) was synthesized based on previous method. The PDDA-RGO was prepared by reducing GO by PDDA. Briefly, the dispersion of GO (60 mg of GO in 20 mL water) was sonicated for 40 min. After that, 800  $\mu$ L of 35 wt% PDDA was added into the dispersion and kept stirring for 10 min. Then the dispersion was heated at 90 °C for 5 h while the color turned from yellow-brown to black. The resulting dispersion was filtered and washed with ultra-pure water for 3 times. The PDDA-RGO was dried under vacuum at 60 °C to become solid samples. Finally, the solid samples were dispersed in ultra-pure water to spread into 0.5 mg mL<sup>-1</sup> PDDA-RGO dispersion.

### 2.3. Preparation of modified electrode

5  $\mu$ L of 0.5 mg mL<sup>-1</sup> PDDA-RGO suspension was dropped onto the cleaned GCE surface and subsequently dried at room temperature. Then 5  $\mu$ L 5 mg mL<sup>-1</sup> BOD or 5  $\mu$ L 10 mg mL<sup>-1</sup> GOD was casted onto the PDDA-RGO/GCE and dried at 4 °C for 4 h. Finally, the BOD/PDDA-RGO/GCE as a biocathode and GOD/PDDA-RGO/GCE as a bioanode were rinsed by ultra-pure water to remove weakly bound molecules and was stored at 4 °C for further use.

5  $\mu$ L 5 mg mL<sup>-1</sup> PVF which has been dispersed in ethanol was dropped onto the PDDA-RGO/GCE and subsequently dried at room temperature. Then 5  $\mu$ L 10 mg mL<sup>-1</sup> GOD was casted onto the PVF/PDDA-RGO/GCE and dried at 4 °C for 4 h. Finally, the GOD/PVF/PDDA-RGO/GCE as a bioanode were rinsed by ultra-pure water to remove weakly bound molecules and was stored at 4 °C for further use.

### 2.4. Instrumentations

A CHI 750D electrochemical workstation (Shanghai, China) was used all over electrochemical experiments. In the experiments to optimize the conditions, a two-electrode configuration was used with a Pt electrode (0.2 mm) as the reference electrode and the bare or modified electrodes as the working electrode. In the experiments to detect glucose by the SPSs, the GOD/PVF/PDDA-RGO/GCE

and BOD/PDDA-RGO/GCE were used as a biocathode and a bioanode, respectively. Open circuit potential ( $V_{oc}$ ) values were recorded. In other experiments, a three-electrode configuration was used with a platinum wire as the auxiliary electrode, a saturated calomel electrode (SCE) as the reference electrode, and the modified or bare GCE electrodes as the working electrode.

### 3. RESULTS AND DISCUSSION

#### 3.1 Electrochemical characterization of GOD/PDDA-RGO /GCE

Firstly, the electrochemical characterization of GOD/PDDA-RGO/GCE without electron mediator has been investigated (Figure 1).

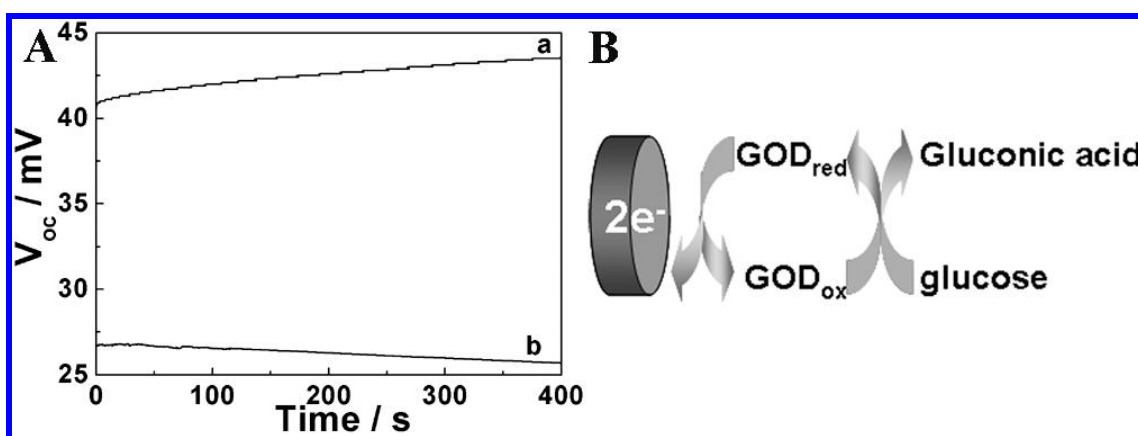


**Figure 1.** (A) The OCP of GOD/PDDA-RGO /GCE in 0.2 M, pH 7.0 PBS in the (a) absence and (b) presence of 10 mM glucose. (B) Schematic illustration of GOD/PDDA-RGO /GCE catalyzing glucose without mediator.

As shown in Figure 1A, the open circuit potential (OCP) at the GOD/PDDA-RGO /GCE bioanode shifted from 40.8 mV (Figure 1A, curve a) to 27 mV (Figure 1A, curve b) after the addition of 10 mM glucose. This result clearly indicated that the oxidation of glucose catalyzed by GOD resulted in the OCP change. As shown in Figure 1B, with the addition of glucose, glucose was catalyzed into gluconic acid by  $GOD_{ox}$  (oxidized state) which has been modified on the electrode surface and  $GOD_{ox}$  itself has been transformed into  $GOD_{red}$  (reduced state) to result in the increase of  $GOD_{red}$ . Then, a large number of  $GOD_{red}$  lost electrons via PDDA-RGO to oxidize into  $GOD_{ox}$ , resulting in the electrons gradually increased on the electrode surface. In the two-electrode system, no current between the electrodes occurred and accordingly the electrons gradually accumulated on the anode electrode surface, which resulted in the decrease of anode electrode potential.[14, 28, 43] The mechanism could be shown as following:



## 3.2 Signal amplification of ferrocene for GOD/PDDA-RGO /GCE

The electrocatalytic response of GOD/PDDA-RGO /GCE to glucose after the addition of the electron mediator (Fc) using the three-electrode configuration was investigated (Figure 2A). Figure 2A showed the cyclic voltammograms (CVs) of the GOD/PDDA-RGO /GCE bioanode with and without the addition of 10 mM glucose in 0.2 M, pH 7.0 PBS containing 10 mM  $\text{Fc}(\text{COOH})_2$  at  $100 \text{ mV s}^{-1}$ . In the absence of glucose, two pairs of redox peak at 0.45 V and 0.55 V were observed, resulting from  $\text{Fc}(\text{COOH})_2$  reversible transition on the electrode surface (Figure 2A, curve a) and it indicated that the electron mediator can achieve electron transfer at the electrode surface. After the addition of 10 mM glucose, a remarkable increase in the anodic current and an obvious decrease in the cathodic current were found, indicating the efficient oxidation of glucose (Figure 2A, curve b).

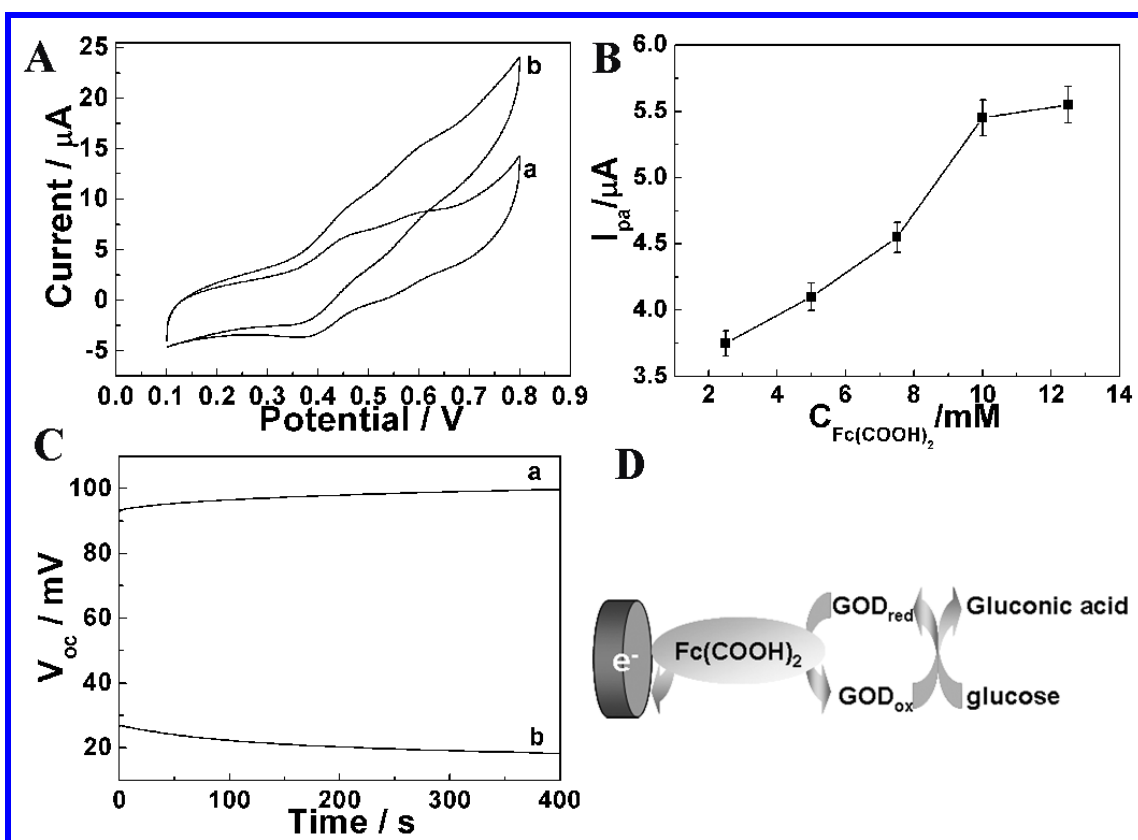


**Figure 2.** (A) The CVs of the GOD/PDDA-RGO /GCE bioanode without (curve a) and with (curve b) 10 mM glucose in 0.2 M, pH 7.0 PBS containing 10 mM  $\text{Fc}(\text{COOH})_2$  at  $100 \text{ mV s}^{-1}$ . (B) The CVs of the GOD/PDDA-RGO /GCE bioanode under different concentrations of  $\text{Fc}(\text{COOH})_2$  in 0.2 M, pH 7.0 PBS at  $100 \text{ mV s}^{-1}$ . (C) The OCP of GOD/PDDA-RGO /GCE in 0.2 M, pH 7.0 PBS containing 10 mM  $\text{Fc}(\text{COOH})_2$  in the (a) absence and (b) presence of 10 mM glucose. (D) Schematic illustration of GOD/PDDA-RGO /GCE catalyzing glucose with  $\text{Fc}(\text{COOH})_2$ .

As shown in Figure 2D, glucose was catalyzed into gluconic acid by  $\text{GOD}_{ox}$  and the produced  $\text{GOD}_{red}$  was oxidized by the  $\text{Fc}(\text{COOH})_2$  subsequently. The  $\text{Fc}(\text{COOH})_2$  has been oxidized on the electrode surface and lost a large number of electrons to lead to the increase of anodic current. It

indicated that the  $\text{Fc}(\text{COOH})_2$  has involved in the electron transfer of GOD.[44, 45] The mechanism could be shown as following:



Then, the effects of  $\text{Fc}(\text{COOH})_2$  concentration on the performance of the GOD/PDDA-RGO /GCE were investigated as shown in Figure 2B. Figure 2B showed the plot of the  $\text{Fc}(\text{COOH})_2$  concentration versus the CVs response of GOD/PDDA-RGO /GCE. With the increasing of  $\text{Fc}(\text{COOH})_2$  concentration from 2.5 mM to 10 mM, the oxidation peak current increased gradually because  $\text{Fc}(\text{COOH})_2$  involved in the electron transfer of GOD. When the more  $\text{Fc}(\text{COOH})_2$  existed in a solution, the more its conduction electrons, the stronger the electrochemical amplification in a certain range. When the  $\text{Fc}(\text{COOH})_2$  concentration has been increased to 12.5 mM, the oxidation peak current trended to an almost constant value. Therefore, the 10 mM  $\text{Fc}(\text{COOH})_2$  was used for the experiments.

As shown in Figure 2C, the OCP at the GOD/PDDA-RGO /GCE bioanode with 10 mM  $\text{Fc}(\text{COOH})_2$  shifted from 92 mV (Figure 2C, curve a) to 28 mV (Figure 2C, curve b) after the addition of 10 mM glucose, which indicated that the  $V_{\text{oc}}$  of GOD/PDDA-RGO /GCE with  $\text{Fc}(\text{COOH})_2$  has a larger change than that without  $\text{Fc}(\text{COOH})_2$  after added the same 10 mM glucose. Therefore, it proved that the  $\text{Fc}(\text{COOH})_2$  has a nice signal amplification for the glucose detection.

### 3.3 Signal amplification of PVF in the GOD/PVF/PDDA-RGO/GCE

It has been reported that the electron mediator modified on the electrode surface could participate in electron transfer and amplify current signals due to close contact with the electrode.[46, 47] Therefore, the PVF polymer containing ferrocene has been introduced to modify the electrode surface. The CVs and OCP has been used to evaluate the amplification ability of PVF (Figure 3). As shown in Figure 3A, without the addition of glucose to solution, a pair of well-defined and quasi-reversible redox peaks (Figure 3A, curve a) that originated from the PVF on the electrode were observed and it proved the PVF achieved a good electron transfer on the electrode surface. After addition of 10 mM glucose, the shape of the CVs at GOD/PVF/PDDA-RGO/GCE electrode distinctly changed and an obvious increasing in the oxidation peak current was found; at the meantime, the reduction peak current was decreased (Figure 3A, curve b).

As shown in Figure 3D, glucose has been catalyzed to glucose acid by  $\text{GOD}_{\text{ox}}$  and then the produced  $\text{GOD}_{\text{red}}$  has been oxidized to  $\text{GOD}_{\text{ox}}$  by PVF. Finally, a large number of  $\text{PVF}_{\text{red}}$  has been oxidized to  $\text{PVF}_{\text{ox}}$  on the electrode surface. The results demonstrated that the immobilized GOD molecules were bioactive and still maintained their natural biocatalytic activities toward their substrate, glucose. The PVF could effectively amplify the signal. The mechanism could be shown as following:



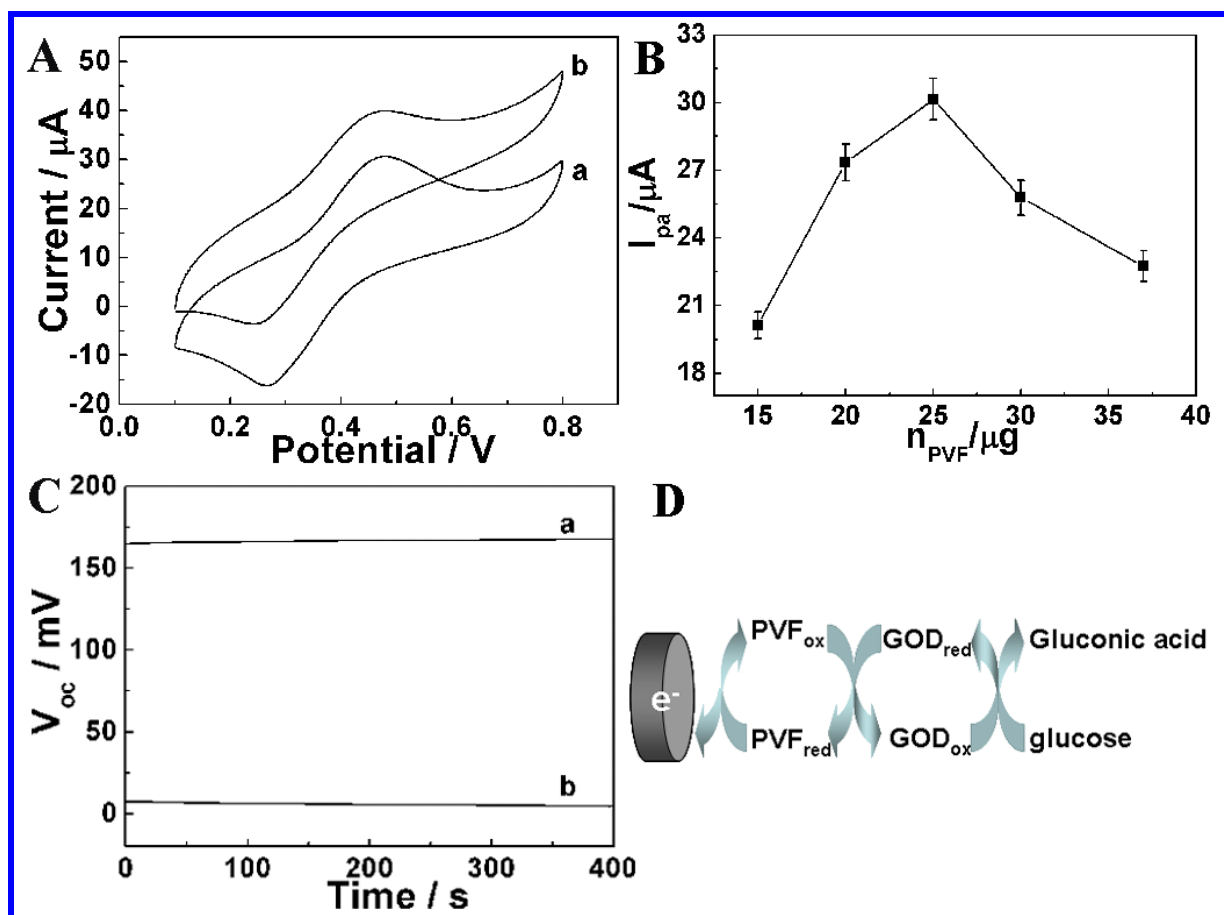


**Figure 3.** (A) The CVs of the GOD/PVF/PDDA-RGO/GCE bioanode without (curve a) and with (curve b) 10 mM glucose in 0.2 M, pH 7.0 PBS at  $100 \text{ mV s}^{-1}$ . (B) The CVs of the GOD/PVF/PDDA-RGO/GCE bioanode under different concentrations of PVF in 0.2 M, pH 7.0 PBS at  $100 \text{ mV s}^{-1}$ . (C) The OCP of GOD/PVF/PDDA-RGO/GCE in 0.2 M, pH 7.0 PBS in the (a) absence and (b) presence of 10 mM glucose. (D) Schematic illustration of GOD/PVF/PDDA-RGO/GCE catalyzing glucose.

The amount of PVF on the GOD/PVF/PDDA-RGO/GCE was optimizingd as shown in Figure 3B. As the amount of PVF on the GOD/PVF/PDDA-RGO/GCE increased from  $15 \mu\text{g}$  to  $25 \mu\text{g}$ , the oxidation peak current gradually increased and more than  $25 \mu\text{g}$ , the current response began to decrease because the PVF layer was too thick to hinder the electronic transmission between GOD and electrode surface. Therefore, the  $15 \mu\text{g}$  PVF has been selected as the optimal conditions for the following experiments.

The GOD/PVF/PDDA-RGO/GCE was further investigated by the OCP catalytic response to glucose as shown in Figure 3C. With the addition of 10 mM glucose, the OCP at the GOD/PVF/PDDA-RGO/GCE electrode changed from 168 V (Figure 3C, curve a) down to 8 V (Figure 3C, curve b), indicating the largest response for the glucose detection.

### 3.4 Electrocatalytic response of BOD/PDDA-RGO/GCE towards $O_2$

It is well known that the BOD can be used as a biocatalyst to selectively catalyze the four-electron reduction of oxygen.[48-50] The direct electron transfer (DET) of BOD at an electrode modified by various carbon materials such as highly oriented pyrolytic graphite, porous carbonaceous, carbon nanotubes (CNTs), carbon spheres, and plastic-formed carbon has been reported. In this study, the BOD/PDDA-RGO/GCE electrode was constructed as a biocathode for reduction of  $O_2$ . Figure 4 showed the CVs of BOD/PDDA-RGO/GCE electrode in  $N_2$  (Figure 4, curve a), air (Figure 4, curve b), and oxygen (Figure 4, curve c)-saturated PBS (pH 7.0). As shown in Figure 4, a significant reduction current was observed at -0.55 V in oxygen-saturated PBS (pH 7.0). The reduction current in oxygen-saturated PBS (curve c) was larger than that in air-saturated PBS (pH 7.0) and  $N_2$ -saturated PBS (pH 7.0) (Figure 4, curve a), suggesting that reduction currents observed at BOD/PDDA-RGO/GCE resulted from BOD-catalyzed oxygen reduction. This result further demonstrated that the BOD was successfully modified on the BOD/PDDA-RGO/GCE and retained good biological activity (BOD-catalyzed  $O_2$  reduction can be realized).

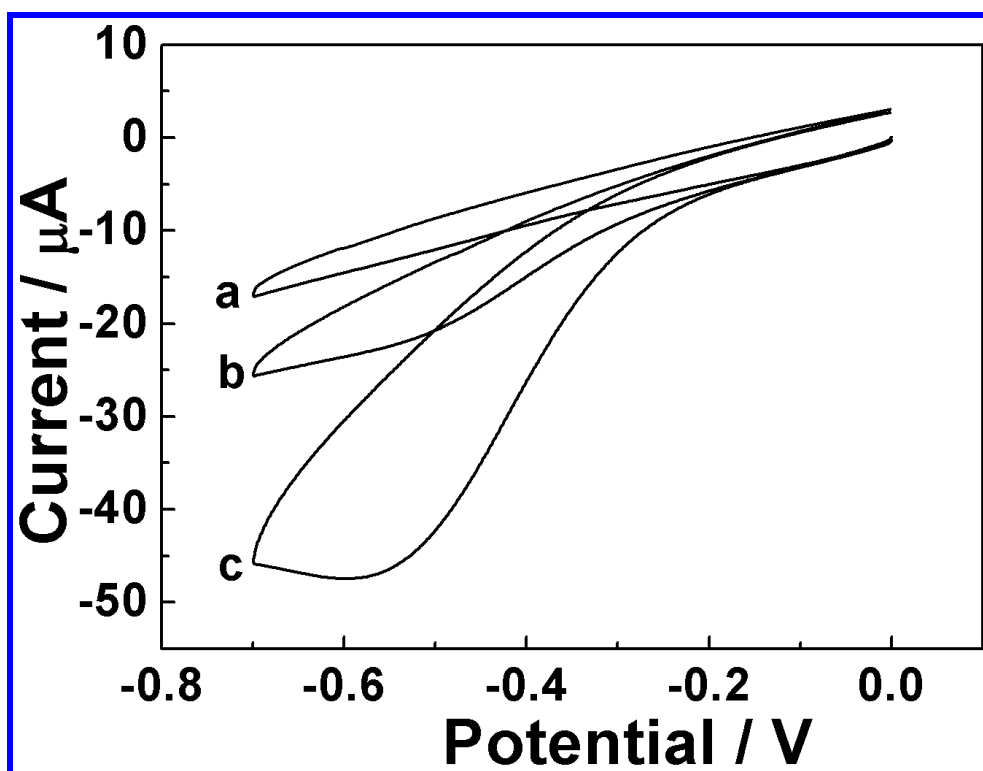
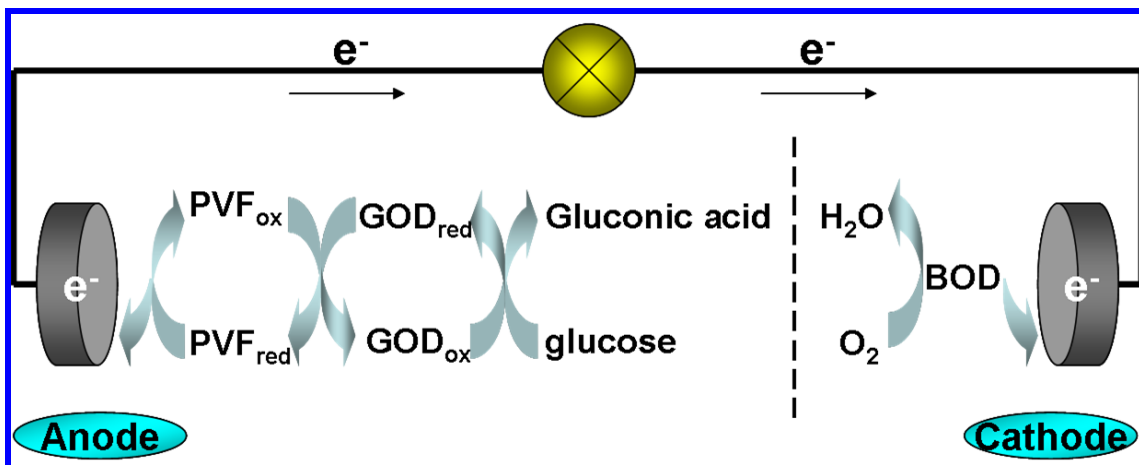


**Figure 4.** CVs of GOD/PVF/PDDA-RGO/GCE under nitrogen (a), air (b), or oxygen (c)-saturated PBS (pH 7.0) with a scan rate of  $100 \text{ mV s}^{-1}$ , respectively.

### 3.5 Self-powered biosensors for glucose detection

Using the GOD/PVF/PDDA-RGO/GCE as a bioanode and the BOD/PDDA-RGO/GCE as a biocathode, a SPS was successfully developed as shown in Scheme 1.



**Scheme 1.** Schematic illustration of the SPSs fabricated by using the GOD/PVF/PDDA- RGO/GCE as a bioanode and BOD/PDDA-RGO/GCE as a biocathode..

In the bioanode, GOD<sub>ox</sub> was used as a biocatalyst for bioelectrocatalytic oxidation of glucose to gluconic acid and GOD<sub>ox</sub> itself has been reduced to GOD<sub>red</sub>. Then, GOD<sub>red</sub> has been oxidized by PVF and PVF<sub>red</sub> was oxidized on the electrode surface to release the electron. In the biocathode, dissolved O<sub>2</sub> intercepted the glucose oxidation-derived electrons from the bioanode, and it should react with the cathodic enzyme (BOD) and be reduced into water under normal circumstances (Scheme 1). As a result, the amount of electron transfer from the bioanode to the biocathode was based on the amount of glucose, which was used as SPSs for glucose sensing.

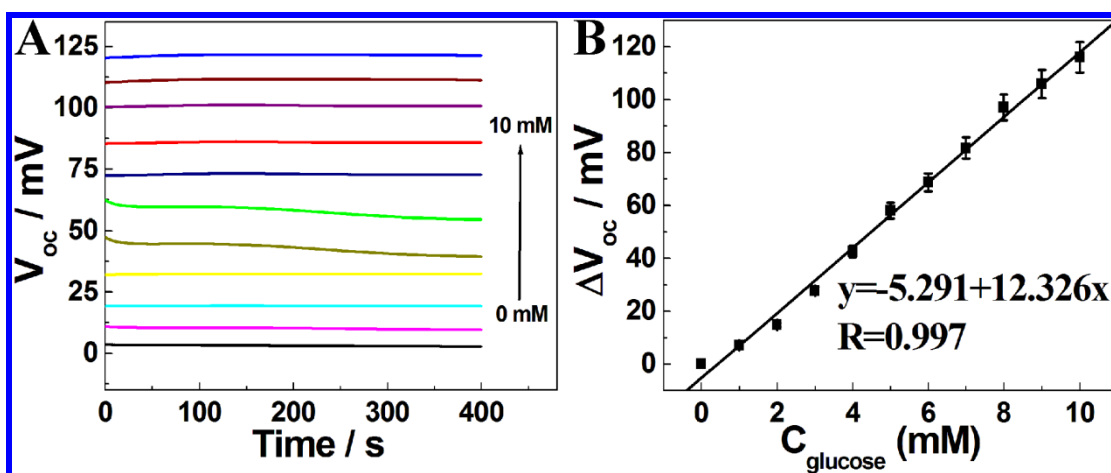


**Figure 5.** (A) The OCP of the SPSs with different concentration of glucose in 0.2 M, pH 7.0 PBS. (B) The calibration curve of glucose detection.

For the detection of glucose, a glucose solution with various concentrations was added into the SPSs. The OCP of the SPSs was recorded until a stable response was observed. The data was shown in Figure 5. As shown in Figure 5A, with the increasing concentration of glucose, the OCP increased gradually. That is because with the addition of glucose, the bioanode potential decreased gradually,

while the biocathode potential was essentially kept constant. The difference was measured and increased as the increase of glucose. Figure 5B showed the calibration curve, in which the increase of  $\Delta$ OCP value (the difference between OCP of the SPSs in the absence of glucose and OCP of the SPSs in the presence of glucose) increased linearly with the increasing glucose concentration ranging from 0.1mM to 10 mM ( $R^2 = 0.997$ ). The linear range of our method was comparable to those reported for other electrochemical sensors as shown in Tabel 1. The low detection limit was estimated to be 23.7  $\mu$ M glucose (S/N =3). Therefore, the method was sensitive and facile for glucose detection, which could promise the possibility of its application in real samples.

**Table 1.** Comparison analytical performance of glucose biosensor based on the GOD catalysis.

Glucose biosensors	Linear range (mmol L <sup>-1</sup> )	Detecting limit ( $\mu$ mol L <sup>-1</sup> )	Ref.
GOD/PVA-Au-pphTEOS	1.0~8.0	0.7	[51]
Nafion-MGF-GOD / GCE	1.0~12.0	250	[52]
GOD/MWCNT-CS	1.0~10.0	20	[53]
GOD/ERGO/poly-Lysine.	0.25~5	-	[54]
GOD-Nafion/GaHCF-CILPE	0.2~6.0	50	[55]
GOD/BSA/AuNP-PbNW/Pt	0.05~2.2	2	[56]
GOD/GCS/NCNTs	0.048~0.857	-	[57]
Self-powered glucose biosensor	0.1~10	23.7	This work

#### 4. CONCLUSION

In summary, by using the PDDA-RGO to immobilize the GOD and BOD well, the GOD/PVF/PDDA-RGO/GCE as a bioanode and BOD/PDDA-RGO/GCE as a biocathode were successfully used to build the bioelectrocatalysis-based SPSs for the sensing of glucose. The CVs and OCP has been used to explore the electron transport on the bioanode and biocathode surface. The electronic mediator has been introduced for electrochemical signal amplification. It was found that the electronic mediator not only could have a good current signal amplification of the bioanode, but also could effectively enlarge their potential signal. Furthermore, the electronic mediator has been modified on the electrode surface is superior to the electronic mediator was in solution.

#### ACKNOWLEDGMENTS

This work was financially supported by Natural Science Foundation of Jiangxi Province (20142BAB203101 and 20143ACB21016), the Ground Plan of Science and Technology Projects of Jiangxi Educational Committee (KJLD14023), the Open Project Program of Key Laboratory of Functional Small Organic Molecule, Ministry of Education, Jiangxi Normal University (No. KLFS-KF-201410; KLFS-KF-201416) and Innovation Foundation for Graduate Student of Jiangxi Province and Jiangxi Normal University (YC2014-S159).

## References

1. L. Liu, Q. Ma, Y. Li, Z. Liu, X. Su, *Biosens. Bioelectron.*, 63 (2015) 519.
2. J.X. Yu, S. M Matthews, K. Yunus, J. G Shapter, A. C Fisher, *Int. J. Electrochem. Sci.*, 8 (2013) 1849.
3. C. Ye, X. Zhong, R. Yuan, Y. Chai, *Sens. Actuators, B*, 199 (2014) 101.
4. P. Yang, L. Wang, Q. Wu, Z. Chen, X. Lin, *Sens. Actuators, B*, 194 (2014) 71.
5. H. Yang, W. Wei, S. Liu, *Spectrochimica acta. Part A, Mol. Biomol. Spectros.*, 125 (2014) 183.
6. Y. Song, H. Liu, H. Tan, F. Xu, J. Jia, L. Zhang, Z. Li, L. Wang, *Anal. Chem.*, 86 (2014) 1980.
7. Y. Liu, M. Yuan, L. Qiao, R. Guo, *Biosens. Bioelectron.*, 52 (2014) 391.
8. F.-Y. Kong, S.-X. Gu, W.-W. Li, T.-T. Chen, Q. Xu, W. Wang, *Biosens. Bioelectron.*, 56 (2014) 77.
9. M. Moumene1, A. Tabet-Aoull1, M. Gougis, D. Rochefort, M.Mohamed, *Int. J. Electrochem. Sci.*, 9 (2014) 176
10. J. Tian, Q. Liu, C. Ge, Z. Xing, A.M. Asiri, A.O. Al-Youbi, X. Sun, *Nanoscale*, 5 (2013) 8921.
11. Y. Song, J. Chen, H. Liu, Y. Song, F. Xu, H. Tan, L. Wang, *Electrochim. Acta* , 158 (2015) 56.
12. M. Zhao, Y. Gao, J. Sun, F. Gao, *Anal Chem*, 87 (2015) 2615.
13. Q. Liu, Y. Yang, H. Li, R. Zhu, Q. Shao, S. Yang, J. Xu, *Biosens. Bioelectron.*, 64 (2015) 147.
14. Y.Y. Yu, Z.G. Chen, S.J. He, B.B. Zhang, X.C. Li, M.C. Yao, *Biosens. Bioelectron.*, 52 (2014) 147.
15. J. Yoshimoto, N. Tanaka, M. Inada, R. Arakawa, H. Kawasaki, *Chem. Lett.*, 43 (2014) 793.
16. Q. Xu, S.-X. Gu, L. Jin, Y.-e. Zhou, Z. Yang, W. Wang, X. Hu, *Sens. Actuators, B*, 190 (2014) 562.
17. G.-X. Zhong, W.-X. Zhang, Y.-M. Sun, Y.-Q. Wei, Y. Lei, H.-P. Peng, A.-L. Liu, Y.-Z. Chen, X.-H. Lin, *Sens. Actuators, B*, 212 (2015) 72.
18. Y. Zhang, E. Zhou, Y. Li, X. He, *Anal. Methods*, 7 (2015) 2360.
19. X. Zhang, Q. Liao, S. Liu, W. Xu, Y. Liu, Y. Zhang, *Anal. Chim. Acta*, 858 (2015) 49.
20. J. Zhang, J. Ma, S. Zhang, W. Wang, Z. Chen, *Sens. Actuators, B*, 211 (2015) 385.
21. Q. Wang, Q. Wang, M. Li, S. Szunerits, R. Boukherroub, *RSC Advances*, 5 (2015) 15861.
22. P.M. Nia, W.P. Meng, F. Lorestani, M.R. Mahmoudian, Y. Alias, *Sens. Actuators, B*, 209 (2015) 100.
23. Y. Liu, S. Liu, R. Chen, W. Zhan, H. Ni, F. Liang, *Electroanalysis*, 27 (2015) 1138.
24. M. Li, C. Han, Y. Zhang, X. Bo, L. Guo, *Anal. Chim. Acta*, 861 (2015) 25.
25. B. Haghighi, B. Karimi, M. Tavahodi, H. Behzadnia, *Mater. Sci. Eng., C*, 52 (2015) 219.
26. X. Zhang, Q. Liao, M. Chu, S. Liu, Y. Zhang, *Biosens. Bioelectron.*, 52 (2014) 281.
27. X. Xiao, J. Ulstrup, H. Li, M.e. Wang, J. Zhang, P. Si, *Electrochim. Acta*, 130 (2014) 559.
28. M. Wooten, S. Karra, M. Zhang, W. Gorski, *Anal. Chem.*, 86 (2014) 752.
29. L.-M. Liu, J. Wen, L. Liu, D. He, R.-y. Kuang, T. Shi, *Anal. Biochem.*, 445 (2014) 24.
30. Y.Q. Zhang, Y.J. Fan, L. Cheng, L.L. Fan, Z.Y. Wang, J.P. Zhong, L.N. Wu, X.C. Shen, Z.J. Shi, *Electrochim. Acta*, 104 (2013) 178.
31. J. Chen, R. Zhu, J. Huang, M. Zhang, H. Liu, M. Sun, L. Wang, Y. Song, *Analyst* (2015).
32. D. Zhu, T. Hu, Y. Zhao, W. Zang, L. Xing, X. Xue, *Sens. Actuators, B*, 213 (2015) 382.
33. L. Zhang, Y. Wang, C. Ma, P. Wang, M. Yan, *RSC Advances*, 5 (2015) 24479.
34. C. Hou, S. Fan, Q. Lang, A. Liu, *Anal. Chem.*, 87 (2015) 3382.
35. M. Zhou, J. Wang, *Electroanalysis*, 24 (2012) 197.
36. D. Wen, L. Deng, S. Guo, S. Dong, *Anal. Chem.*, 83 (2011) 3968.
37. M.T. Meredith, S.D. Minter, *Anal. Chem.*, 83 (2011) 5436.
38. R.L. Arechederra, S.D. Minter, *Anal. Bioanal. Chem.*, 400 (2011) 1605.
39. W. Zheng, H.Y. Zhao, J.X. Zhang, H.M. Zhou, X.X. Xu, Y.F. Zheng, Y.B. Wang, Y. Cheng, B.Z. Jang, *Electrochem. Commun.*, 12 (2010) 869.

40. J. Halamek, T.K. Tam, G. Strack, V. Bocharova, M. Pita, E. Katz, *Chem. Commun. (Camb)*, 46 (2010) 2405.
41. E. Katz, A.F. Bückmann, I. Willner, *JACS*, 123 (2001) 10752.
42. N. Kakehi, T. Yamazaki, W. Tsugawa, K. Sode, *Biosens. Bioelectron.*, 22 (2007) 2250.
43. Y.-F. Gao, T. Yang, X.-L. Yang, Y.-S. Zhang, B.-L. Xiao, J. Hong, N. Sheibani, H. Ghourchian, T. Hong, A.A. Moosavi-Movahedi, *Biosens. Bioelectron.*, 60 (2014) 30.
44. A.A. Ensafi, H. Karimi-Maleh, *J. ElectroAnal. Chem.*, 640 (2010) 75.
45. Y. Liang, H. Liu, K. Zhang, N. Hu, *Electrochim. Acta*, 60 (2012) 456.
46. P.E. Erden, C. Kacar, F. Ozturk, E. Kilic, *Talanta*, 134 (2015) 488.
47. N.F. Atta, A. Galal, S.H. Hassan, *Int. J. Electrochem. Sci.*, 10 (2015) 2265.
48. L. Zhang, M. Zhou, S. Dong, *Anal. Chem.*, 84 (2012) 10345.
49. S. Tsujimura, Y. Kamitaka, K. Kano, *Fuel cells*, 7 (2007) 463.
50. P. Ramírez, N. Mano, R. Andreu, T. Ruzgas, A. Heller, L. Gorton, S. Shleev, *BBA-Bioenergetics*, 1777 (2008) 1364.
51. U. Lad, G.M. Kale, R. Bryaskova, *Anal. Chem.*, 85 (2013) 6349.
52. Y. Wang, H.X. Li, J.L. Kong, *Sens. Actuators, B*, 193 (2014) 708.
53. B.Y. Wu, S.H. Hou, M. Yu, X. Qin, S. Li, Q. Chen, *Mater. Sci. Eng., C*, 29 (2009) 346.
54. L. Hua, X. Wu, R. Wang, *Analyst*, 137 (2012) 5716.
55. B. Haghghi, M. Khosravi, A. Barati, *Mater. Sci. Eng., C*, 40 (2014) 204.
56. H. Wang, X. Wang, X. Zhang, X. Qin, Z. Zhao, Z. Miao, N. Huang, Q. Chen, *Biosens. Bioelectron.*, 25(2009) 142.
57. W. Wei, P.P Li, Y. Li, X.D Cao, S.Q. Liu, *Electrochem. Commun.*, 22 (2012) 181.